Single Thermite-Type Combustion Synthesis of Fe_2VAl for Thermoelectric Applications from Fe, V_2O_5 and Al Powders

Keisuke Abe[1,*], Asami Kikuchi[1,*], Noriyuki Okinaka[2], and Tomohiro Akiyama[2]

[1]Graduate School of Engineering, Hokkaido University, Sapporo 060-8628, Japan

[2]Center for Advanced Research of Energy Conversion Materials, Hokkaido University, Sapporo 060-8628, Japan[1]

Corresponding Author: Tomohiro Akiyama

E-mail address: takiyama@eng.hokudai.ac.jp

Tel.: +81 11 706 6842

Abstract

Single thermite-type combustion synthesis (STCS) for synthesizing Heusler alloy Fe_2VAl from Fe, V_2O_5, and Al powders for thermoelectric applications was proposed and investigated, in which the microstructure and the thermoelectric properties of the product were mainly examined. Macroscopically, STCS was successfully carried out to produce metallic product of Fe_2VAl in lower part and alumina as slag in upper part. According to SEM observation and FE-EPMA-analyzed, elemental mapping images, the product contained dispersed inclusions of spherical Al_2O_3 with 0.4mol% and angulated AlN with 1.0mol%. In comparison to the reported data on Fe_2VAl, the thermal conductivity at room temperature became about half. It could be because of increased phonon scattering due to dispersed AlN&Al_2O_3 and non-stoichiometry of the product; $Fe_{2.06}V_{1.01}Al_{0.93}$. As a result, the maximum values for the product were 99.6 $\mu Wm^{-1}K^{-2}$ in power factor and 2.19×10^{-3} at 309 K in dimensionless figure of merit.

Keywords: thermoelectric materials; microstructure; metals and alloys; composite materials

1. Introduction

Thermoelectric properties are typically evaluated by dimensionless figure of merit, ZT. ZT is expressed as follows;

$$ZT = S^2T/(\rho\kappa) \quad (1)$$

where Z is the figure of merit of a thermoelectric material (K^{-1}), S is the Seebeck coefficient (VK^{-1}), T is the absolute temperature (K), ρ is the electrical resistivity (Ωm), and κ is the thermal conductivity ($Wm^{-1}K^{-1}$). It is essential for thermoelectric materials to improve the ZT.

Fe_2VAl has been known as a thermoelectric material for its unique physical properties. Heusler alloy Fe_2VAl is a semimetal with a narrow pseudogap at the Fermi level [1, 2]. Small stoichiometric deviations can cause big changes in its transport properties [3]. Two methods for controlling the pseudogap in Fe_2VAl have been reported by several researchers. One is to change its composition from stoichiometric to nonstoichiometric [3-5], and the other is to substitute a fourth element [6-13]. The methods proposed increase the absolute values of the Seebeck coefficient and reduce the electrical resistivity of Fe_2VAl [3-13]. However, the thermal conductivity of Fe_2VAl is comparatively large as a thermoelectric material; about 28 ($Wm^{-1}K^{-1}$) at room temperature, resulting in the small ZT of Fe_2VAl [14]. For obtaining high-performance Fe_2VAl, it is essential to decrease its thermal conductivity.

Three processes of Fe_2VAl fabrication have been conventionally reported. The first one is melting method based on ingot metallurgy [3-6, 8-10], the second one is mechanical alloying [11-13], and the third one is the combination of them [7]. All of the conventional processes require pure V as raw material to synthesize Fe_2VAl, in which V has been industrially produced by a thermite reaction from V_2O_5 and Al using strong exothermic reaction. Thermite reactions are reduction reactions of metal oxides using Al as a reduction agent. In these reactions, oxidation of Al to Al_2O_3 releases a large amount of heat, propagating a rapid combustion wave. The problem is that the large exothermic heat generated is only used for producing V, without any heat recovery. In the thermite reaction of the V production, Al is excessively added to eliminate

unreacted V_2O_5, resulting in the low purity V product with Al. For purifying the product, electron beam melting with volatilization of Al is necessary [14]. Next, the V obtained is arc-melted or mechanically alloyed with Fe and Al to synthesize Fe_2VAl as final product. Thus, for synthesizing Fe_2VAl industrially, we concluded that the production method of V has three defects; 1) Exothermic heat from the thermite reaction is not used efficiently. 2) The loss of Al is inevitably accompanied. 3) The following exergy-consuming electron beam melting treatment is needed.

To overcome these drawbacks in the conventional production of Fe_2VAl, thermite-type combustion synthesis (TCS), defined as combustion synthesis using thermite reactions from Fe, V_2O_5 and Al powders, is quite attractive for saving energy and operating time. Excess heat from thermic reaction of $Al+V_2O_5$ is reasonably utilized for melting of Fe and excess Al, and for alloying of Fe_2VAl without the electron beam melting and the loss of Al (see Fig.1). In addition, conventional melting requires all the raw materials—Fe, V, and Al—to be pure metals. In contrast, in the proposed process, we can use metal oxide V_2O_5, which is cheaper and more abundant than V. In addition, TCS for producing Fe_2VAl has possibility of improving its ZT. P. Wen et al. reported that the thermal conductivity of $CoSb_3$ was reduced by dispersion of Al_2O_3, which is a by-product of TCS [15]. If the by-product of Al_2O_3 can be dispersed in the product Fe_2VAl, its thermal conductivity can be reduced, resulting in higher ZT. Therefore, the purpose of this study is to synthesize Heusler alloy Fe_2VAl by thermite-type combustion synthesis, in which its microstructure and thermoelectric properties are mainly examined.

We can define “single thermite-type combustion synthesis” (STCS) as a process for synthesizing Fe_2VAl via one thermite reaction, in which V_2O_5 is reduced by Al. Moreover, we can define “double thermite-type combustion synthesis” (DTCS) as a process involving two thermite reactions, in which both Fe_2O_3 and V_2O_5 are reduced by Al. However, this paper deals with STCS only and DTCS will be reported elsewhere.

2. Experimental

Commercially available powders of Fe with 99.9% in purity and 3–5 μm in grain size, V_2O_5 with 99.99% in purity and 75 μm in grain size, and Al with 99.99% in purity and 3 μm in grain size were used for preparing the samples studied here. The powders were weighed according to the stoichiometry of Eq. (3) and were then mixed in an alumina tumbling ball milling pot, which did not contain any balls to prevent the powders adhering to the inside wall. The milling pot was operated at 100 rpm for 3.6 ks in air. The resulting mixture was then placed in a graphite crucible. A carbon foil igniter was placed on the powders. Finally, the powders were electrically flashed at room temperature for about 10 s. The STCS-synthesized (STCSed) products were homogenized at 1273 K for 172.8 ks in an Ar atmosphere. The phase composition and morphology of the products were determined and analyzed by using an X-ray diffractometer (Miniflex, Rigaku, Tokyo, Japan) and field emission electron probe micro analyzer (FE-EPMA) (JXA-8530F, JEOL, Tokyo, Japan). The STCSed samples were cut to predefined forms. The electrical resistivity and Seebeck coefficient of the samples were measured using a Seebeck coefficient/electrical resistance measurement system (ZEM-3, ULVAC-RIKO, Yokohama, Japan) from room temperature to 873 K in a He atmosphere. The thermal conductivity of the sample was measured by a laser flash thermal constant analyzer (TC-7000, ULVAC-RIKO, Yokohama, Japan) from room temperature to 873 K in vacuum.

3. Results and Discussions

STCS consists of an exothermic reaction (1) and an alloying reaction (2), given below:

$$1/2\ V_2O_5 + 5/3\ Al \rightarrow V + 5/6\ Al_2O_3 \quad (1)$$

$$2\ Fe + V + Al \rightarrow Fe_2VAl \quad (2)$$

Reaction (2) can proceed by utilizing the large amount of exothermic heat generated by reaction (1) (ΔH = –621 kJ at 298 K). The overall reaction of STCS can be written as follows:

$$2\ Fe + 1/2\ V_2O_5 + 8/3\ Al \rightarrow Fe_2VAl + 5/6\ Al_2O_3 \quad (3)$$

The theoretical achieving temperature of a combustion synthesis reaction, which is called adiabatic flame temperature, is very important to estimate the state of the products after reaction. The adiabatic flame temperature of the equation (3) was calculated to be 2327 K which was the same as the melting point of Al_2O_3. From the calculation, we revealed that 60.8% of Al_2O_3 melted and the rest did not melt. This temperature is higher than the melting point of Fe, V, and Al, showing that Fe, V, and Al were liquid during STCS.

Figure 1 shows the schematic illustrations of the conventional V-production method and the proposed STCS method as heat recovery of the conventional thermite reaction. Fe and Al was also added to the raw materials of the conventional V-production method.

Fig. 2 shows the photographs of the samples placed in a graphite crucible before and after STCS. Before STCS, the color of the raw materials resembled that of ash. After STCS, the ash color of the raw materials disappeared, and products with metallic luster and black color were generated. The raw materials and products were subjected to X-ray diffraction (XRD) measurements, the results of which are shown in Fig. 3. The figure indicates that the metallic luster and black products are Fe_2VAl and Al_2O_3, respectively. The degree of ordering was estimated by reference intensity ratio (RIR) method. Fe_2VAl which had ordered L21 structure was about 46.1%, which had BCC structure was about 53.9%. This showed the STCSed Fe_2VAl did not have perfectly ordered L21 structure.

Fig. 4 shows a scanning electron microscope (SEM) image and elemental mapping images of the cross-sectional surface of the STCSed and heat-treated product, respectively. The locations at which Al, O, and N were partially richer correspond to the black parts in the SEM image. These black parts indicate that Al_2O_3 and AlN existed partly in the STCSed and heat-treated product. During STCS, the reaction given by Eq. (3) occurred, and the melted products were separated by gravity. The densities of Fe_2VAl and Al_2O_3 are 6.60×10^3 and 3.97×10^3 kgm^{-3}, respectively. This implies that Fe_2VAl should be at the bottom of the crucible and Al_2O_3 on top of it. Fig. 2 confirms this as the black product (Al_2O_3) was observed in the upper region of the reactor after STCS and the metallic luster product (Fe_2VAl) was observed in the lower region. However, the products were air-cooled and the Fe_2VAl and Al_2O_3 solidified before they could perfectly separate. This resulted in residual Al_2O_3 in Fe_2VAl. AlN could have been produced by the reaction between N_2 left in the powders and Al. From the elemental mapping images in Fig. 4, the contained amounts of Al_2O_3 and AlN were estimated to be about 0.4 and 1.0 mol%, respectively. More detailed SEM image and elemental mapping images of the dotted area of inclusions in Fig. 4 are shown in Fig. 5. The black parts which have circular shape were Al_2O_3 and which have angulated shape were AlN. The reason for the difference in shape between Al_2O_3 and AlN can be considered from the adiabatic flame temperature. The adiabatic flame temperature of the STCS reaction was 2327 K, implying that most part of Al_2O_3 was liquid and AlN was solid. Liquid Al_2O_3 was curled by the effect of surface tension before solidification.

Fig. 6 shows SEM images and elemental mapping images of the matrix part in Fig. 4. In the matrix, we confirmed segregation of V with about 1 μm in size. Fig. 7 shows SEM images and elemental mapping images of V before and after heat treatment for 48 h at 1273 K. Before the homogenization heat treatment, larger segregation of V was observed in the dotted area in Fig. 7(a) and 7(b). During heat treatment, the larger segregation of V became smaller with the diffusion of V but smaller segregation of V was still left. The melting point of V is 2183 K which is higher than that of Fe (1811 K) and Al (933 K), meaning that it was short time for V to maintain the liquid state and that

diffusion was not enough. In addition, the size of V_2O_5 was 75 μm which was larger than that of Fe (3–5 μm) and Al (3 μm). This shows that the inside of the product V cannot be diffused completely. To obtain perfectly homogenized Fe_2VAl, smaller size V_2O_5 and longer heat treatment will be needed.

Table 1 Elemental analysis of the matrix part of STCSed and heat-treated Fe_2VAl, in which upper, middle and lower parts are corresponded to *u, m*, and *l* in Fig. 2.

	Molar ratio (mol%)			Standard variation (mol%)		
	Fe	V	Al	Fe	V	Al
Upper part	50.8	26.0	23.2	0.51	0.72	0.24
Middle part	51.4	25.4	23.2	1.02	1.44	0.44
Lower part	52.3	24.1	23.6	0.69	1.05	0.39
Average	51.5	25.2	23.3	0.94	1.31	0.40

Table 1 shows the results of the quantitative analysis for the matrix part of the STCSed and homogenized Fe_2VAl. The quantitative analysis was taken place for upper part, middle part, and lower part, of the matrix part (except Al_2O_3 and AlN parts) of the STCSed and heat-treated Fe_2VAl to research its compositional difference in the different locations. The upper, middle, and lower part were corresponded to u, m, and l in Fig. 2, respectively. Elemental analysis was taken place ten times at every location on the terms of probe diameter of 5 μm. The composition of the STCSed Fe_2VAl was almost uniform at every vertical position within the standard variation. The average composition of the STCSed Fe_2VAl was 51.5mol%Fe-25.2 mol%V-23.3mol%Al ($Fe_{2.06}V_{1.01}Al_{0.93}$.).

The temperature dependence of electrical resistivity, the Seebeck coefficient, the thermal conductivity, the power factor, and the dimensionless figure of merit of the STCSed and heat-treated Fe_2VAl, together with the reference data (taken from T. Mori et al.), are shown in Fig. 8 [10]. The electrical resistivity showed a downward slope, which agrees with previous studies [10]. The Seebeck coefficient values were about 10% to 30% smaller than those previously reported [10]. This reduction was attributed

to the small difference in the compositions of STCSed and stoichiometric Fe_2VAl. The thermal conductivity at room temperature was about half of that reported in the literature [10]. The reduction of the thermal conductivity is believed to be related to increase of phonon scattering by the increase in grain boundary regions due to dispersed Al_2O_3 and AlN and the small difference of the composition of the STCSed and heat-treated alloy from stoichiometry. The maximum values of power factor and dimensionless figure of merit were 99.6 $\mu Wm^{-1}K^{-2}$ and 2.19 $\times$ 10^{-3}, respectively at 309 K.

This article indicated the possibility of STCS for producing Fe_2VAl, however, further improvement in thermoelectric properties are desired. For larger Seebeck coefficient, the segregation of V should be removed by diminishing the grain size of V_2O_5 and the heat treatment condition should be optimized for obtaining more homogenized and ordered Fe_2VAl; and then substitution of a fourth element is needed.

4. Conclusions

(1) Single thermite-type combustion synthesis was successfully carried out to separate metallic part of Fe_2VAl as product and alumina part macroscopically due to gravitation.

(2) Microscopically, the product contained inclusions which are 0.4mol%-Al_2O_3 of circular shape and 1.0mol%-AlN of angulated shape. SEM image and FE-EPMA-analyzed, elemental mapping images showed the V segregation with the size of 1 μm in the matrix part of the product.

(3) The total average composition of the product was $Fe_{2.06}V_{1.01}Al_{0.93}$ according to elemental analysis.

(4) The thermal conductivity at room temperature was about half of that reported in the literature because of the increase of phonon scattering by the increase in grain boundary regions due to dispersed Al_2O_3 and AlN and the small difference of the composition of the STCSed and heat-treated alloy from stoichiometry. As a result, he maximum values of the power factor and the dimensionless figure of merit for the STCSed Fe_2VAl were 99.6 $\mu Wm^{-1}K^{-2}$ and 2.19×10^{-3} at 309 K, respectively.

References

[1] D. J. Singh, I. I. Mazin, Phys. Rev. B. **57** (1998) 14352/1-5.

[2] R. Weht, W. E. Pickett, Phys. Rev. B. **58** (1998) 6855-6861.

[3] Y. Nishino, H. Kato, M. Kato, U. Mizutani, Phys. Rev. B **63** (2001) 233303/1-4.

[4] Y. Hanada, R. O. Suzuki, K. Ono, J. Alloy. Compd. **329** (2001) 63-68.

[5] C. S. Lue, Y.-K. Kuo, Phys. Rev. B **66** (2002) 085121/1-5.

[6] H. Kato, M. Kato, Y. Nishino, U. Mizutani, S. Asano, J. Japan Inst. Metals **65** (2001) 652-656.

[7] W. Lu, W. Zhang, L. Chen, J. Alloy. Compd. **484** (2009) 812-815.

[8] H. Nakayama, N. Ide, Y. Nishino, Mater. Trans. **49** (2008) 1858-1862.

[9] Y. Nishino, S. Deguchi, U. Mizutani, Phys. Rev. B **74** (2006) 115115/1-6.

[10] T. Mori, N. Ide, Y. Nishino, J. Japan Inst. Metals **72** (2008) 593-598.

[11] M. Mikami, A. Matsumoto, K. Kobayashi, J. Alloy. Compd. **461** (2008) 423-426.

[12] M. Mikami, K. Kobayashi, J. Alloy. Compd. **466** (2008) 530-534.

[13] M. Mikami, S. Tanaka, K. Kobayashi, J. Alloy. Compd. **484** (2009) 444-448.

[14] A. Miyauchi, T. H. Okabe, J. Japan. Inst. Metals **74** (2010) 701-711.

[15] P. Wen, H. Mei, P. Zhai, B. Duan, J. Mater. Eng. Perform. **22** (2013) 3561-3565.

Figure captions

Fig. 1 Schematic images (a); the conventional method for producing V by a thermite reaction and (b); the proposed method of producing Fe_2VAl directly for improving the conventional method in terms of heat recovery.

Fig. 2 Photographs of the samples (a) before and (b) after single thermite-type combustion synthesis (STCS), in which one end of well-mixed powder of Fe, V_2O_5, and Al in a vertically-placed graphite crucible were ignited in argon atmosphere with 5N in purity and 0.1MPa in pressure and the lower product had metallic luster; the upper one had black. The points *u*, *m*, and *l* in the lower side are corresponded to upper, middle, and lower part in Table 1, respectively.

Fig. 3 XRD patterns of the raw materials of Fe, Al and V_2O_5, black product in upper part, and metallic luster product in lower part, demonstrating successful thermite reaction due to gravitational separation.

Fig. 4 Scanning Electron Microscope (SEM) image (a) and FE-EPMA-analyzed, elemental mapping images for element O (b), N (c), Fe (d), V (e), and Al (f) of the STCSed and heat-treated product from Fe: V_2O_5: Al=2: (1/2): (8/3) in molar basis, in which main product contained AlN or Al_2O_3 as inclusion of black particle in SEM according to careful observation. Note that dotted area of inclusion has three elements of Al, N and O, which is enlarged for identification of AlN and Al_2O_3 from shape and element in Fig. 5.

Fig. 5 SEM image (a) of dotted area of inclusion in Fig. 4 and FE-EPMA-analyzed, elemental mapping images for element Al (b), N (c), and O (d) in the matrix of the STCSed and heat-treated product, showing angulated AlN and spherical Al_2O_3 due to melting.

Fig. 6 SEM image (a) of matrix without inclusion, and FE-EPMA-analyzed, elemental mapping images for element Fe (b), V (c), and Al (d) of the cross-sectional surface of the STCSed and heat-treated product, showing one micrometer in segregation although it was heat-treated at 1273K for 48 hours.

Fig. 7 Effect of heat-treatment on element V; SEM images (a) of product before heat treatment for 48 h at 1273 K, and (c) product after heat treatment, together with FE-EMPA-analyzed, elemental mapping images (b) and (d) for V. Remember that dotted-area of V disappeared by the heat treatment.

Fig. 8 Temperature dependence of the electrical resistivity, the Seebeck coefficient, the thermal conductivity, the power factor, and the dimensionless figure of merit, of the STCSed and heat-treated Fe_2VAl, which was actually $Fe_{2.06}V_{1.01}Al_{0.93}$ according to elemental analysis. Closed point and dotted line as reference are Fe_2VAl fabricated by arc melting [10].

A) Conventional $V_2O_5 + 5/3Al = 2V + 5/6Al_2O_3 + 621kJ$

$T_{ad} = 3418K$

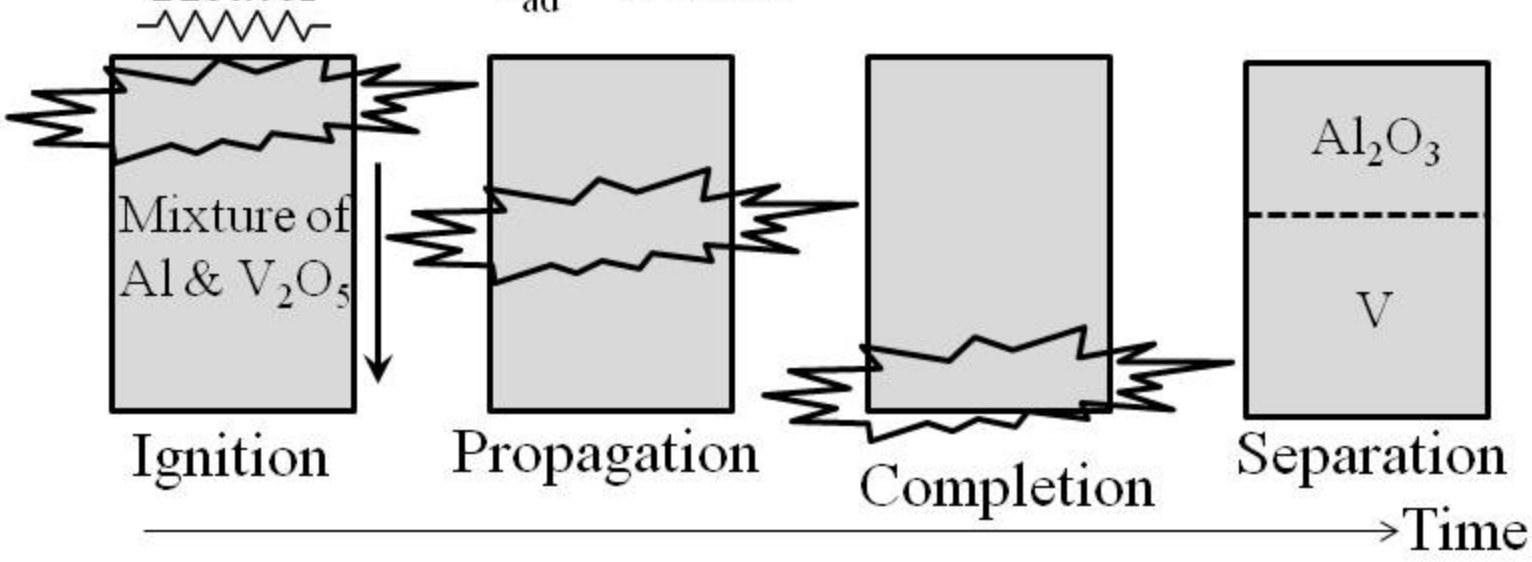

B) Proposed $2Fe + 1/2V_2O_5 + 8/3Al \rightarrow Fe_2VAl + 5/6Al_2O_3$

$T_{ad} = 2327\ K$

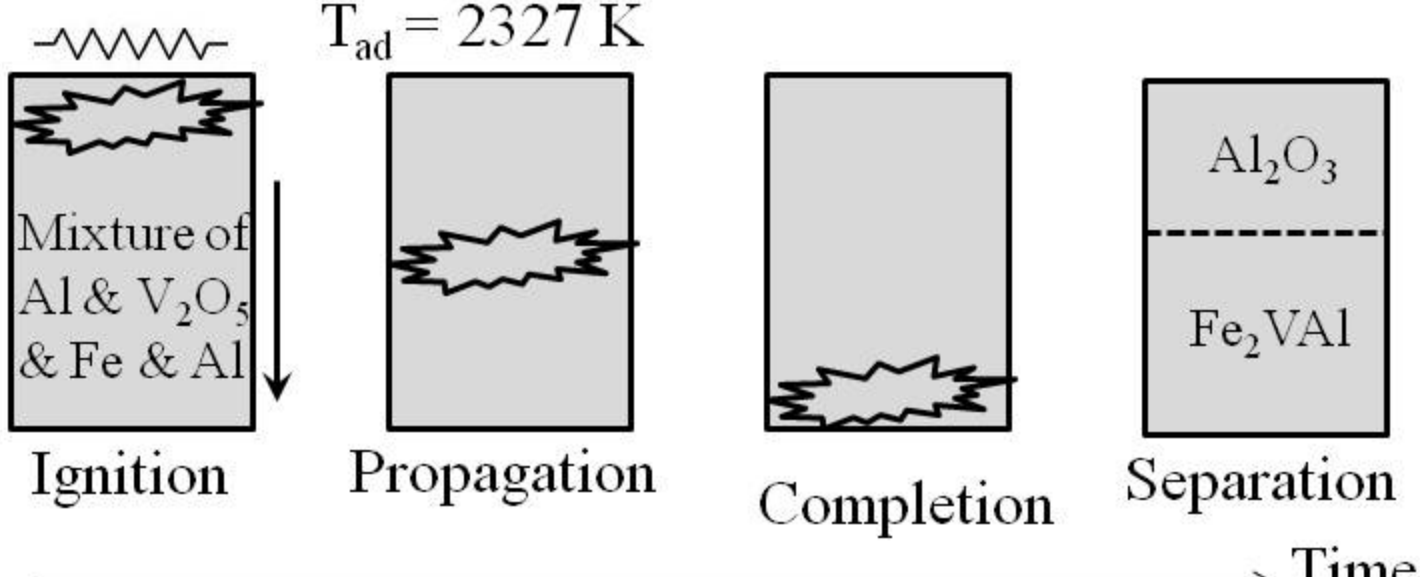

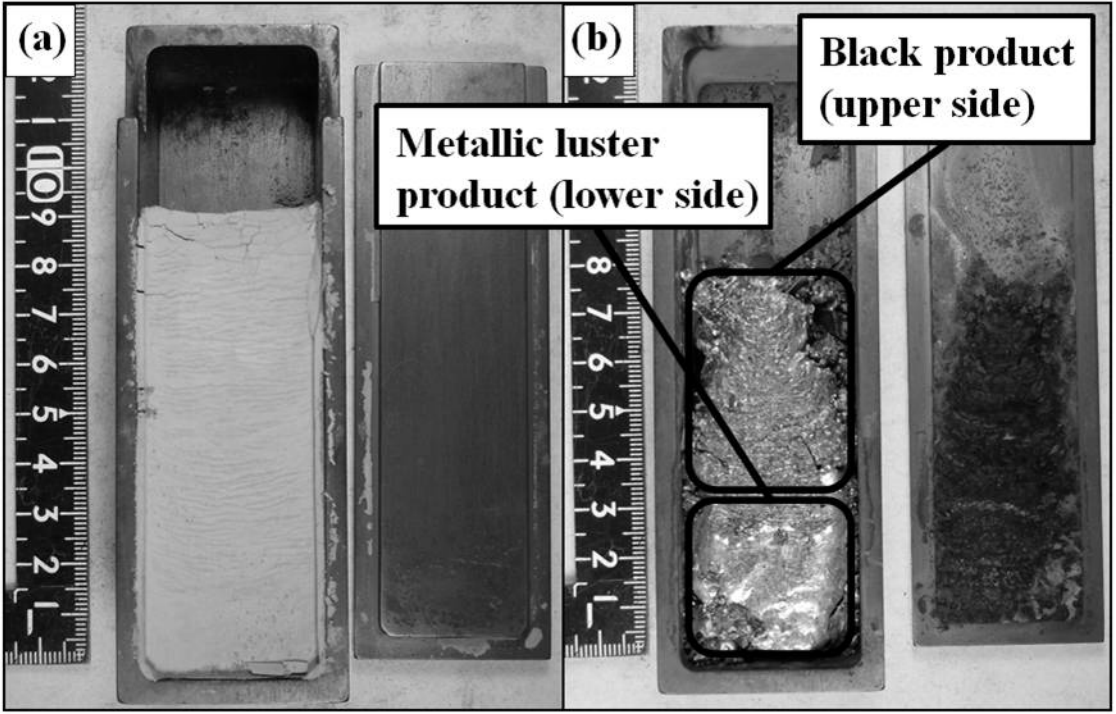
(a)
(b)
Black product
(upper side)
Metallic luster
product (lower side)

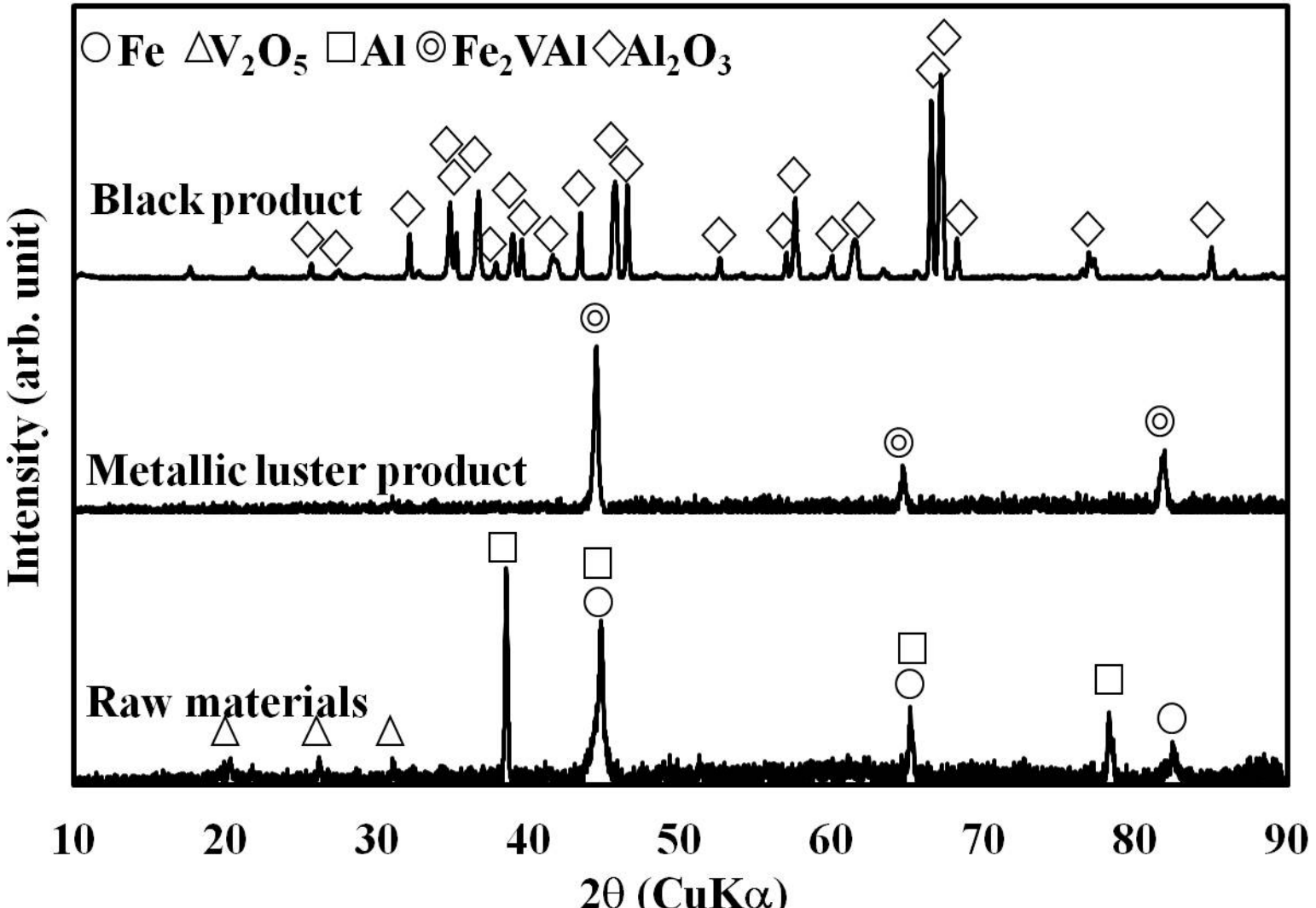
○Fe △V_2O_5 □Al ◎Fe_2VAl ◇Al_2O_3
Black product
Metallic luster product
Raw materials
Intensity (arb. unit)
10
20
30
40
50
60
70
80
90
2θ (CuKα)

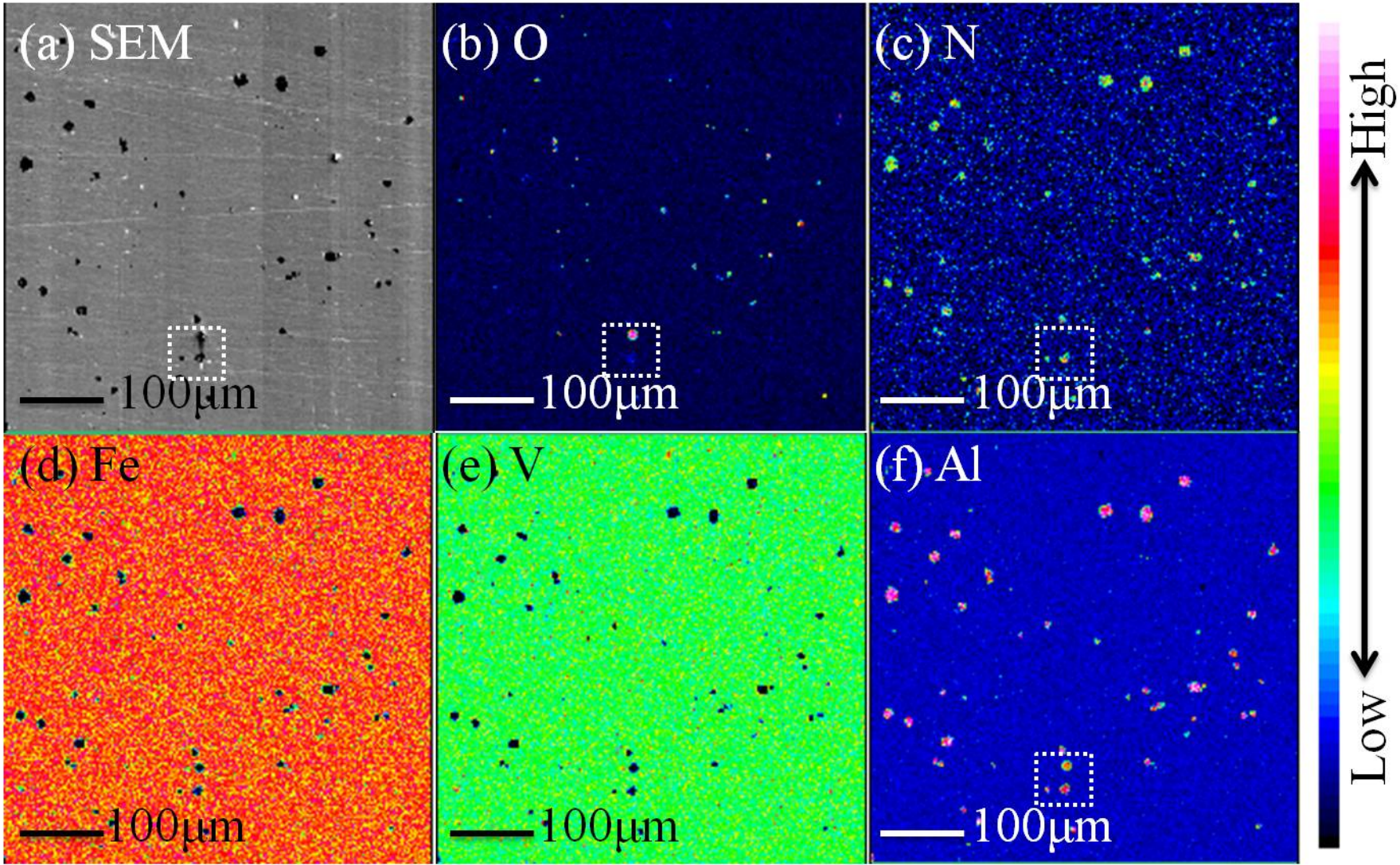
(a) SEM
100μm
(b) O
100μm
(c) N
100μm
(d) Fe
100μm
(e) V
100μm
(f) Al
100μm
High
Low

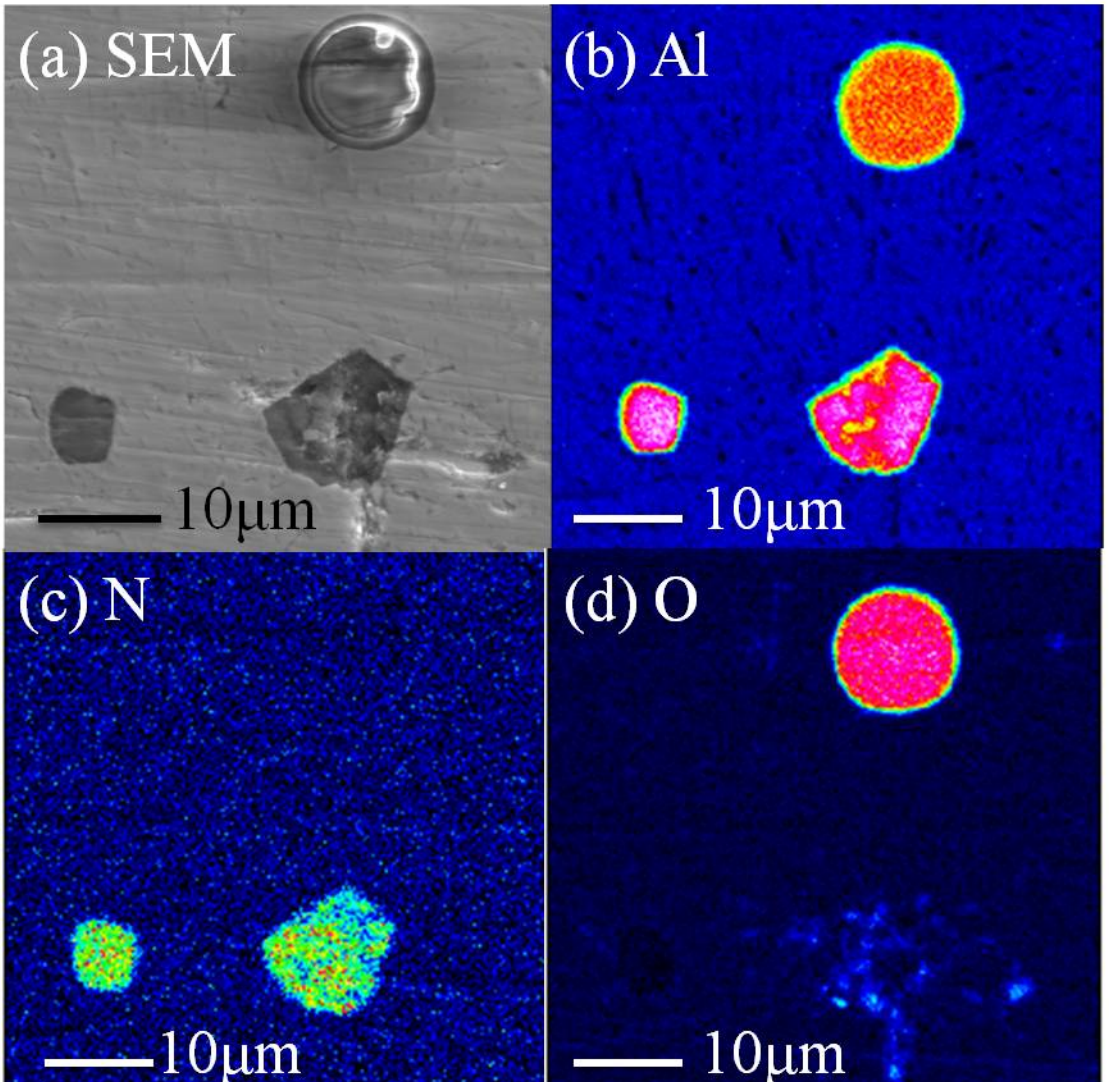
(a) SEM
10μm
(b) Al
10μm
(c) N
10μm
(d) O
10μm
High
Low

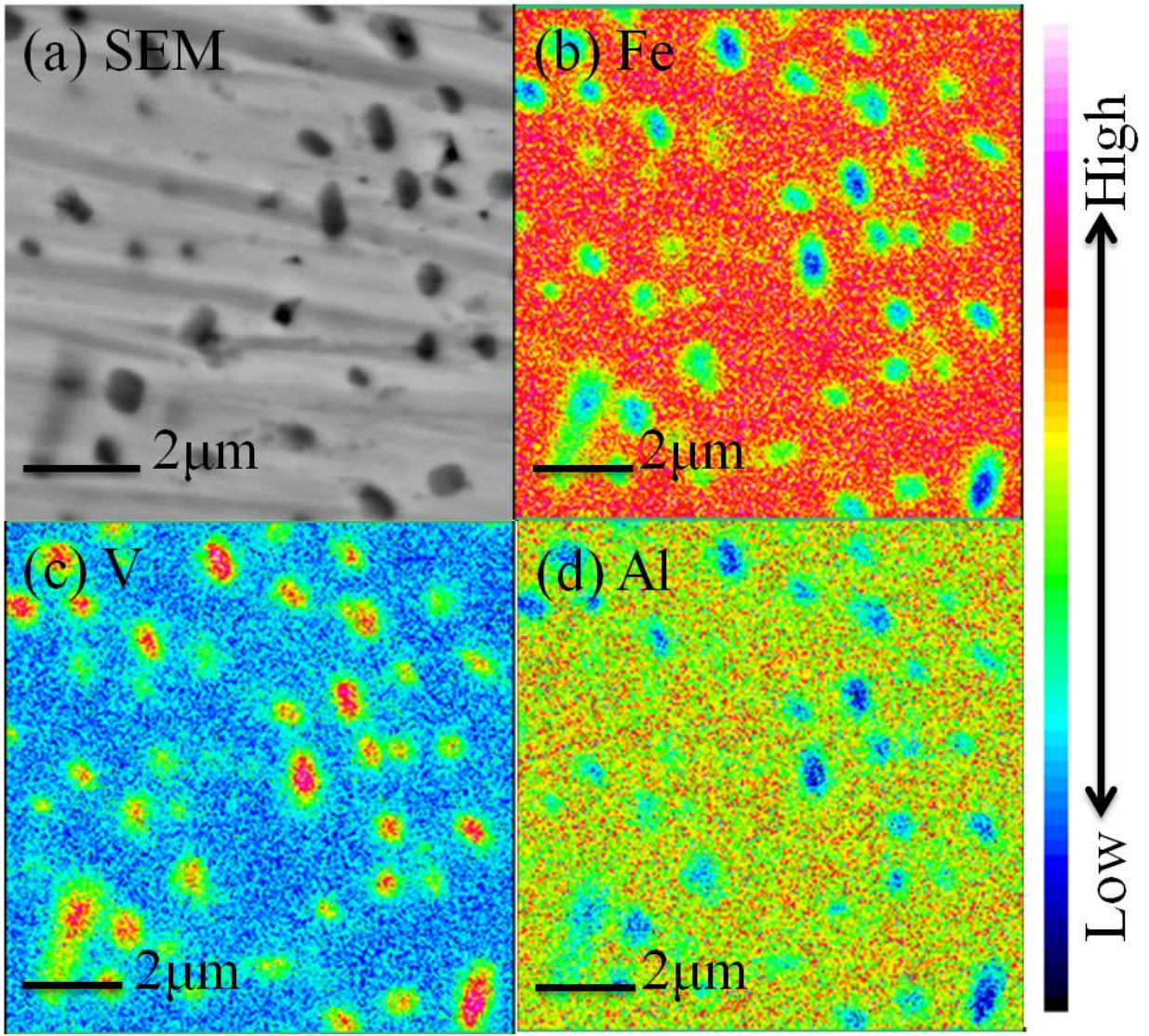
(a) SEM
2μm
(b) Fe
2μm
(c) V
2μm
(d) Al
2μm
High
Low

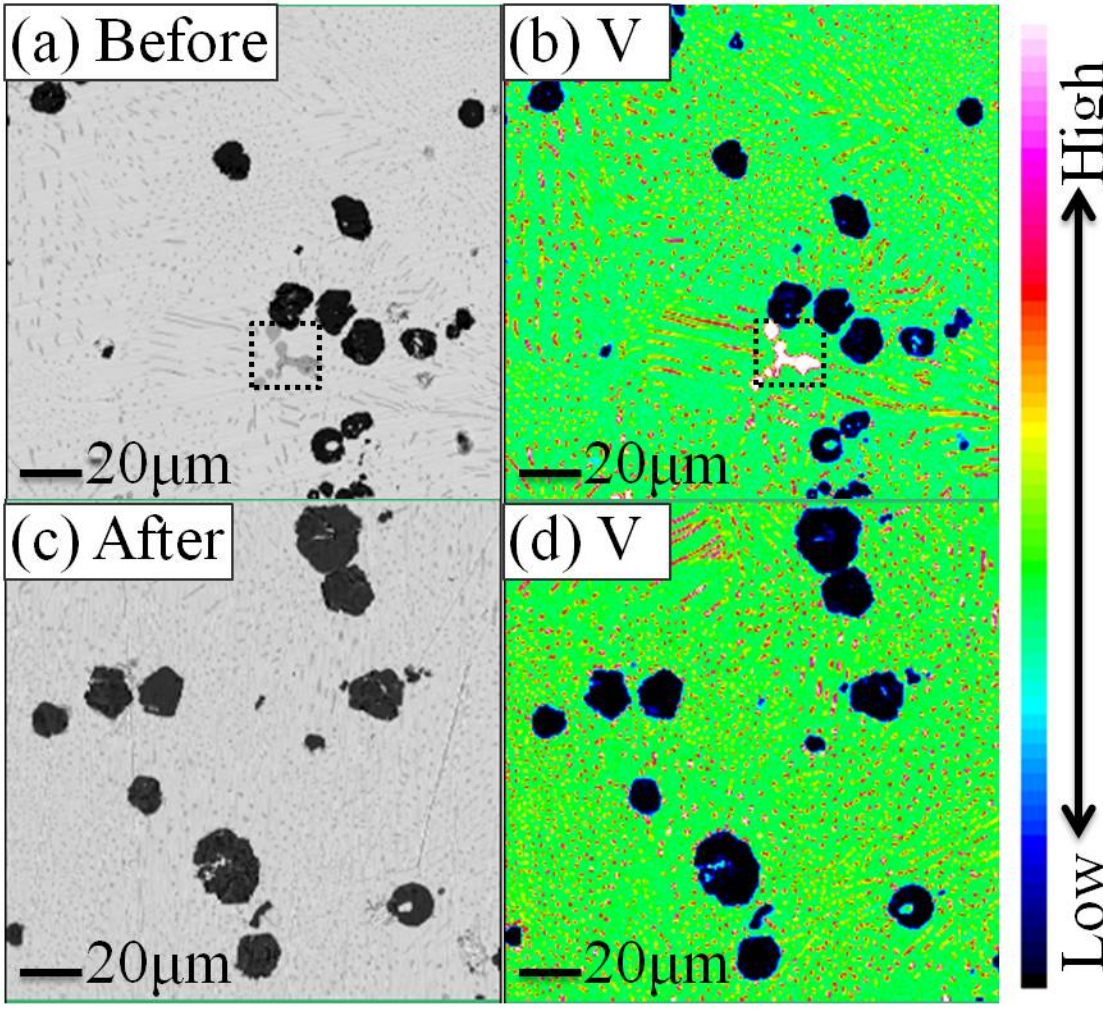
(a) Before
20μm
(b) V
20μm
(c) After
20μm
(d) V
20μm
High
Low

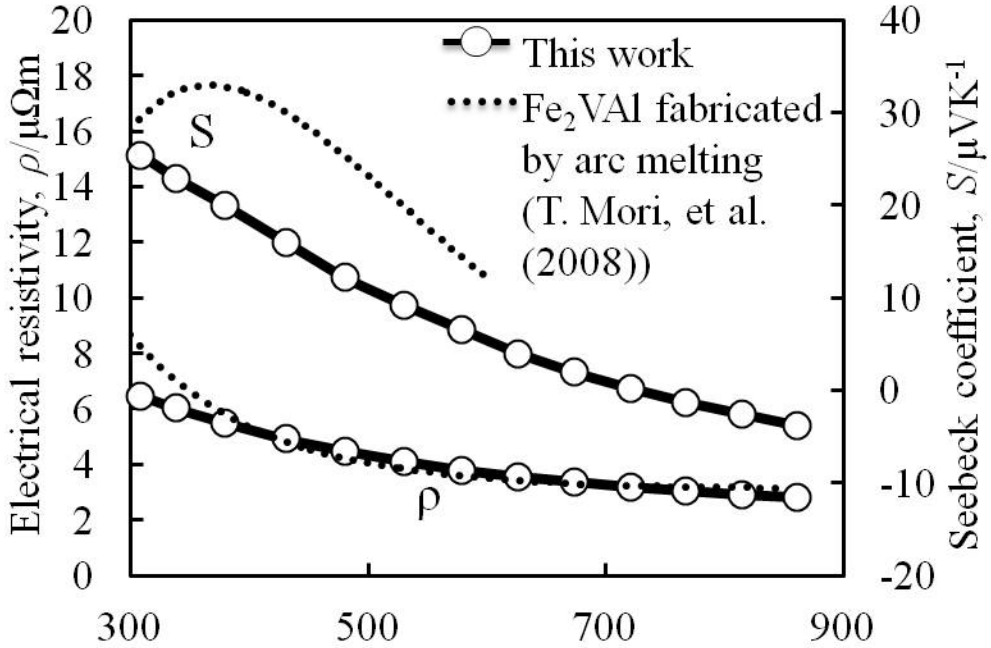
This work
Fe2VAl fabricated by arc melting (T. Mori, et al. (2008))
S
ρ
Electrical resistivity, ρ/μΩm
Seebeck coefficient, S/μVK-1

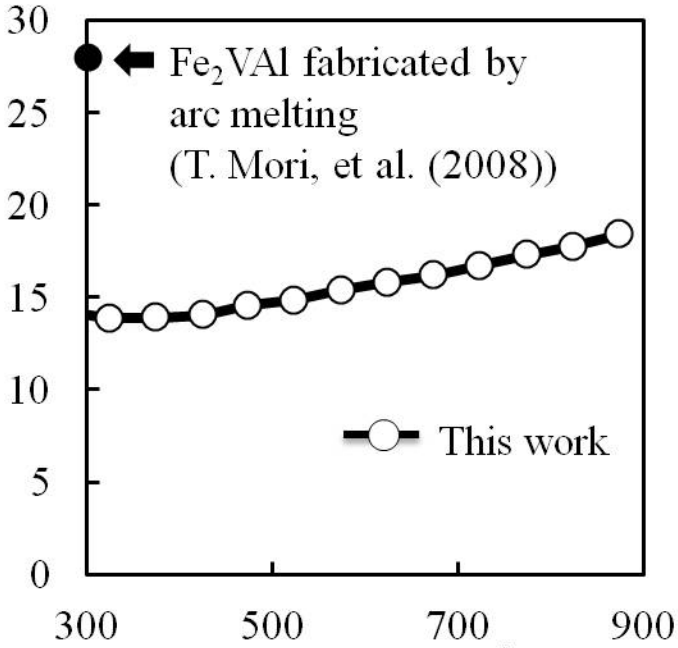
Fe2VAl fabricated by arc melting (T. Mori, et al. (2008))
This work

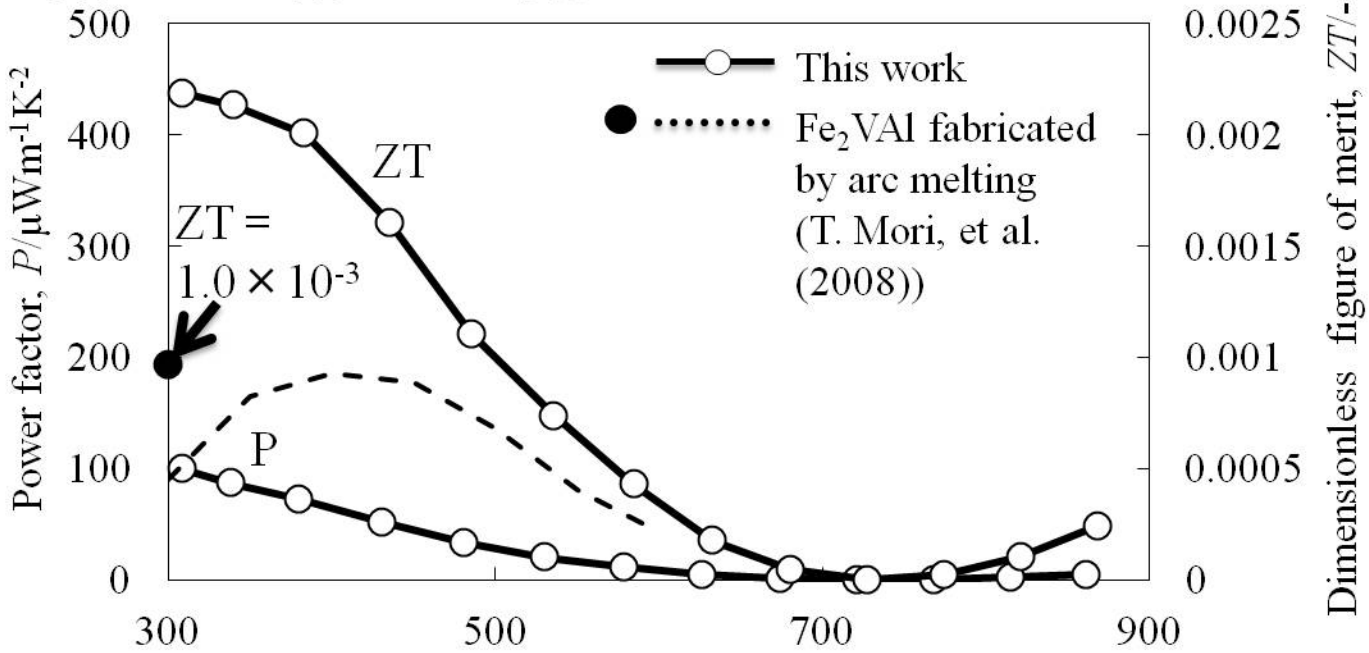
This work
Fe2VAl fabricated by arc melting (T. Mori, et al. (2008))
ZT
ZT = 1.0 × 10-3
P
Power factor, P/μWm-1K-2
Dimensionless figure of merit, ZT/-